Published in final edited form as:

Physiol Meas. 2015 October ; 36(10): 2057–2067. doi:10.1088/0967-3334/36/10/2057.

Compact DD generator-based neutron activation analysis (NAA) system to determine fluorine in human bone *in vivo*: a feasibility study

Farshad Mostafaei[1], **Scott P Blake**, **Yingzi Liu**, **Daniel A Sowers**, **Linda H Nie**

School of Health Sciences, Purdue University, West Lafayette, IN 47907, USA

Abstract

The subject of whether fluorine (F) is detrimental to human health has been controversial for many years. Much of the discussion focuses on the known benefits and detriments to dental care and problems that F causes in bone structure at high doses. It is therefore advantageous to have the means to monitor F concentrations in the human body as a method to directly assess exposure. F accumulates in the skeleton making bone a useful biomarker to assess long term cumulative exposure to F. This study presents work in the development of a non-invasive method for the monitoring of F in human bone. The work was based on the technique of *in vivo* neutron activation analysis (IVNAA). A compact deuterium-deuterium (DD) generator was used to produce neutrons. A moderator/reflector/shielding assembly was designed and built for human hand irradiation. The gamma rays emitted through the $^{19}F(n,\gamma)^{20}F$ reaction were measured using a HPGe detector. This study was undertaken to (i) find the feasibility of using DD system to determine F in human bone, (ii) estimate the F minimum detection limit (MDL), and (iii) optimize the system using the Monte Carlo N-Particle eXtended (MCNPX) code in order to improve the MDL of the system. The F MDL was found to be 0.54 g experimentally with a neutron flux of 7×10^8 n s^{-1} and an optimized irradiation, decay, and measurement time scheme. The numbers of F counts from the experiment were found to be close to the (MCNPX) simulation results with the same irradiation and detection parameters. The equivalent dose to the irradiated hand and the effective dose to the whole body were found to be 0.9 mSv and 0.33 μSv, respectively. Based on these results, it is feasible to develop a compact DD generator based IVNAA system to measure bone F in a population with moderate to high F exposure.

Keywords

fluorine; neutron activation analysis (NAA); deuterium-deuterium (DD) generator; human bone; Monte Carlo simulation (MCNP)

Introduction

Fluorine (F) is an essential trace element in human bone. However, the effects and risks of exposure to fluoride have been controversial. Fluoride can cause different effects in the body

[1]Author to whom all correspondence should be addressed. fmostafa@purdue.edu.

based on the amount ingested; including useful effects at low dosages. There is evidence that fluoridated drinking water has a positive effect on dental caries (Limeback 1999) and is found to be useful in health prevention strategies for both tooth and bone at the proper dosages. Because of these beneficial effects to the human health, there have been recommendations made to add F supplements in approximate level of 1 mg L^{-1} (1 mg F ion per liter of drinking water) to drinking water (Burt 1992). However, when the F concentration exceeds normal values, F toxicity can cause osteosclerosis, osteopenia and/or osteomalacia in an individual's bone mass (Tamer *et al* 2007, Wang *et al* 2007). F toxicity can also cause thyroid hormone imbalance in children (Susheela *et al* 2005), and can also result in joint aches, bone and teeth deformation, calcification of ligaments and impairment in range of motion (Wilson 1993, Shashi *et al* 2008). Dental and bone fluorosis are two consequences of overexposure to fluoride. In the late 1930s, skeletal fluorosis was identified as a widespread disease in India, Africa, and China and many parts of the globe in individuals who consumed drinking water with F concentrations in the range of 3 to >20 mg L^{-1} (Boivin *et al* 1989, Khandare *et al* 2005). In addition to deleterious effects on bones and teeth, consumption of high quantities of fluoride can cause abdominal pain, diarrhea, fatigue, drowsiness, coma, cardiac arrest, and eventually be fatal for humans (Kaminsky *et al* 1990, Whitford 1990, Augenstein *et al* 1991, ATSDR 2003).

The main sources of fluoride exposure include, but are not limited to, fluoridated toothpaste, fluoridated mouthwash, marine products, tea and drinking water (Johnson *et al* 2007, Kurland *et al* 2007, Yadav *et al* 2007). Adults consume 2–3 liters of water per day, which would result in about 2–3 mg F from drinking water per day from the supplements. In addition, individuals over the age of twelve roughly ingest 0.4 mg of F from food per day (Burt 1992). This comes from food cooked in fluoridated water and also from uptake of fluoride in plants and animals (Burt 1992, Whitford 1994).

The F ingested is absorbed in the body primarily through the stomach and small intestine, with slight additional absorption through the mouth (Whitford 1989). Studies suggest that half of ingested fluoride is absorbed within thirty minutes; the plasma peak concentration is therefore reached in the first hour (Phipps 1996). Also, studies demonstrate that the typical bone F concentration in people exhibits a linear relationship with water concentration (Zipkin *et al* 1960, Turner *et al* 1995). Overall, 90% of the consumed F is retained in the body and the remaining 10% is excreted through the feces. F is tightly bound and stored in the skeleton because it displaces the hydroxide (OH^-) functional group in the hydroxyapatite matrix in the bone (Whitford 1994). F accumulates over time in bone and since 99% of the F mass is linked with calcified tissues, concentrations are expected to be highest in the bone. Therefore, bone is a perfect location in the human body to measure F (Whitford 1994).

One way to obtain F concentration in bone is through bone biopsy. However, bone biopsies are not only inconvenient, but also pose a risk to the subject (Krishnan *et al* 1985). X-ray fluorescence (XRF) and neutron activation analysis (NAA) have been used to determine elemental concentrations in bone and other human tissues *in vivo* for over three decades (Ludlow *et al* 2007). X-ray fluorescence (XRF) is not a suitable method to measure F since the highest characteristic x-ray energy for F is 0.677 keV, which is too low to be detected outside of the body (Chettle 2006). NAA is a better choice because of the high natural

abundance of ^{19}F, relatively high neutron capture cross section of ^{19}F, and high energy of the emitted γ-ray to penetrate the tissue. In human IVNAA studies the tissue of interest must be irradiated with a radioactive neutron source or neutron generator while minimizing the radiation dose to the subject (Chettle *et al* 1984). Neutrons in the tissue activate elements and the decay gammas can be detected with a scintillation or semiconductor detector. In the case of F, its presence is detected by measuring the decay of its radioactive daughter. The level of the element can be quantified by comparing the signals between the person and appropriate calibration standards. In this study, F was measured by neutron activation analysis via the $^{19}F(n,\gamma)^{20}F$ reaction. ^{20}F β^- decays (100%) to an excited state of ^{20}Ne, which de-excites 99.1% of the time by the emission of a 1.63 MeV gamma ray (Tilley *et al* 1998).

$$^{19}\mathrm{F} + \mathrm{n} \rightarrow ^{20}\mathrm{F} \rightarrow ^{20}\mathrm{Ne}^* + \beta^- \rightarrow ^{20}\mathrm{Ne} + \gamma$$

This gamma-ray is detected and compared to the signal from calibration standards.

In all the studies using IVNAA to measure element concentrations in bone, hand bone was chosen as a suitable site for several reasons. First, a hand can be extended away from the body, so the torso can be kept out of the neutron beam as much as possible. This reduces the radiation dose to the more radiosensitive organs of the body which are located in the torso. Additionally, no active bone marrow is contained in the adult hand bone which further reduces stochastic radiation risk (ICRP 2002). Another consideration is that it is easy to position a hand inside an irradiation cavity or detection chamber. Finally, people find it psychologically acceptable to have their hand irradiated while they do not, for example, find the idea of a skull irradiation to be equally acceptable.

The IVNAA has been used for F measurements in previous studies, which were performed using a hand irradiation system located at the McMaster University (Mostafaei *et al* 2013a, 2013b, 2015b). In this current study, all irradiations were performed using a compact DD neutron generator at Purdue University. This facility was initially designed and used for studies of manganese and aluminum which are described extensively in the literature (Liu *et al* 2013, 2014). The advantages of a compact DD neutron generator in comparison to McMaster's accelerator include requiring only a small space for the system and its portability. Also, shielding around the generator is designed to be reassembled easily.

Using these data, we had five goals:

1. Determine the feasibility of bone F measurements using a DD neutron generator; and develop the technique of IVNAA for the measurement of F using an optimized moderator, reflector and shielding assembly for hand irradiation.
2. Validate the MCNP results with experiment by using a series of known F concentration phantoms.
3. Determine the F minimum detection limit (MDL).
4. Calculate the equivalent and effective dose using the Monte Carlo simulation.

5. Finally, determine the system requirement for the detection of F in general population with an acceptable radiation dose.

Method and materials

Monte Carlo simulation

The Monte Carlo N-Particle eXtended (MCNPX) code, developed by Los Alamos National Laboratory (LANL) was used in this study. MCNP code was found to be a powerful tool to simulate the particle transport and interactions with matter, including neutrons and photons (http://mcnp.lanl.gov/). The activation, neutron flux, and radiation dose can be tallied with the latest cross sectional data from MCNP code, based on defined source, shielding, reflector, and moderator geometry and composition. The DD source was simulated as a surface source and the hand with bone and two layers of soft tissue was simulated as a sandwich of 10×20 cm^{-2} dimensions. The bone and soft tissue thicknesses were obtained from ICRP23 and were chosen to be 1 cm and 0.5 cm respectively (ICRP 1975). The generator head and its dimensions were modeled as provided by the manufacturer. Phantoms with varying amounts of F (0.82, 1.9, 2.2, 3.2, 6.3, 9.5 and 12.8 g F) were simulated. The fm4 card was used to obtain the probability of the activated nucleus. A 500 ppm F phantom (μgr F/ gr phantom) was modeled and used for further optimization.

Irradiation facility

In this study, all irradiations were performed using a hand irradiation system located at the Purdue University. The DD generator (customized DD-109 manufactured by Adelphi Technology Inc. (Redwood, CA)) produces neutrons via the ($^2D + {}^2D \rightarrow {}^4He \rightarrow {}^3He + n$) fusion reaction and was driven by an ion beam supplied by a radio frequency driven ion source.

This facility was initially designed and used for the study of manganese, which is described in our previous papers (Liu *et al* 2013, 2014).

The main components of a DD neutron generator include ion source, ion extractor, beam target, power supply/electronics rack, and heat exchanger. While the system was operating, deuterium (D_2) gas was provided continuously through a compressed deuterium gas bottle, attached adjacent to the system. Two pumps (roughing and turbo) were used to maintain the gas line and the generator head at a high vacuum. The system's V-shaped target was made from titanium coated copper and provides for efficient neutron generation. Active cooling was maintained to stabilize the titanium surface temperature, which maximizes the neutron production and extends the lifetime of the target. . The generator can produce a neutron flux of up to 3×10^9 n s^{-1}. The neutron flux can be adjusted by changing the acceleration voltage and ion current, which may vary from 80 kV to 125 kV, and 10 mA to 13 mA respectively.

Detection system

The hyper-pure germanium (HPGe) detector (GMX90P4-ST, 100% efficiency) was used as a detection system in this study. The detection system was placed near the irradiation cavity during the measurement because of the short half-life (11.2 s) of F. The detection system is

surrounded by lead blocks to reduce counts from background photons. The DSPEC Plus digital box was used for signal processing, and Maestro γ-ray spectroscopy software was used for signal collection. The system was calibrated using a calibration source with known activity.

Spectrum analysis

A fitting function was used to extract the F peak areas from each phantom spectrum. The peaks were modelled by Gaussian functions and the background by a linear function. The Levenberg-Marquardt fitting algorithm was used for curve fitting and the analysis was programmed by Matlab. The fitting function had a total of five parameters (three for the Gaussian peak and two for the linear background) and took the form:

$$y = mx + b + \frac{a}{\sigma_1\sqrt{2\pi}}\exp\left(-\frac{1}{2}\left(\frac{x - x_a}{\sigma_1}\right)^2\right)$$

Where, y is the count rate (s^{-1}), m represents the slope of the linear background, b the intercept of linear background, a the peak areas, σ_1 the peak width (standard deviation), and x_a the peak centroid. The peak width and centroid position were constrained to fall within 0.5 standard deviations of the values determined from the highest concentration peaks, in order to keep stability of all the fits.

Minimum detectable limit (MDL)

In the literature, there is more than one definition of MDL (Hibbert *et al* 2006). In our laboratory, MDL is calculated in two ways. A simplified way is: $\mathrm{MDL} = \frac{2 \times \sqrt{B}}{C}$

Where B is the background counts under the F γ-ray peak for the zero concentration phantom and C is the slope of the regression line of F counts versus F concentration (Nie *et al* 2011).

A more conservative way to calculate σ_F is to take into account the uncertainties introduced by calibration: $MDL = 2.\ \sigma_F$

$$\left(\frac{\sigma_F}{\mathrm{F}}\right)^2 \approx \left(\frac{(\sigma_A)^2 + (\sigma_C)^2}{(\mathrm{A} - \mathrm{C})^2}\right) + \left(\frac{\sigma_B}{\mathrm{B}}\right)^2 - 2\frac{\sigma_A\sigma_B}{\mathrm{AB}}\rho_{\mathrm{AB}},$$

where σ_F is the measurement uncertainty of the zero concentration phantom, A is the zero concentration phantom peak area, B is the slope, C is the intercept of the calibration line, σ_A, σ_B and σ_C are standard deviations of A, B and C respectively, and ρ_{AB} is the covariance between A and B (Bevington 2003).

Results

Number of counts determined by Monte Carlo (MC) simulation

Based on the MC simulation results, an optimized moderator, reflector, shielding system was built to create a cavity for the irradiation of human hands. The optimized configuration includes tightly fit polyethylene moderator with a 5 cm thickness at the hand irradiation side and an 8 cm graphite reflector. The shielding is chosen and modeled with 15 cm polyethylene, 5 cm borated polyethylene, and 0.5 cm lead. To shield the bremsstrahlung x-rays generated by the electrons emitted back to the plasma source from the primary ion interaction at the titanium target, 8 mm thick lead was placed around the generator head. When the neutrons produced at the target pass through the moderator, the average neutron energy is reduced to thermal and epithermal energies. At this point the neutron capture cross sections are much higher for F in the hand. The reflector is employed to scatter neutrons back into the center of the cavity, increasing the thermal flux per incident neutron, thus making more efficient use of the generated neutrons. The shielding walls provide further neutron and gamma ray shielding to the subject's body (Liu *et al* 2014, Sowers *et al* 2015).

Figure 1 shows the cross section of the irradiation cavity with all optimized layers of moderator, reflector and shielding.

Using fm4 card in MCNPX simulation, the number of the activated nucleus per neutron in a defined volume can be obtained. In combination with the neutron activation analysis equation, the number of F characteristic γ-ray counts from the phantoms with different amount of F (0.82, 1.9, 2.2, 3.2, 6.3, 9.5 and 12.8 g F) were calculated as:

$$\text{Number of counts} = R \times N_0 \times \varepsilon \times \theta \times F_n \times S \times D \times C \quad (1)$$

Where, R is the reaction rate, N_0 is the number of atoms for the target nuclide, ε is the detector efficiency, θ is the branch ratio of the characteristic γ-ray for the specific radionuclides produced, F_n is the neutron flux per second, S is the saturation factor, D is the decay factor, and C is the counting factor.

The detector efficiency was calculated to be 0.0187 for F γ-ray energy at 1.63 MeV. The number of counts from different amount of F is demonstrated in table 1.

The F phantom calibration line using Monte Carlo simulation is shown in figure 2. All the results have relative uncertainties of less than 5%.

Number of counts and MDL determined by experiment

In order to evaluate the Monte Carlo simulation results, F phantoms with various amounts (0.82, 1.9, 2.2, 3.2, 6.3 and 12.8 g) of ammonium fluoride (NH_4F) were prepared. The samples were irradiated in the irradiation cavity for 20 s, transferred to detection system in 8 s, and measured for 30 s with the HPGe γ-ray detection system. The number of counts experimentally is in the same range as MCNPX estimates to within the uncertainties in the phantoms with lower F contents, but it was found to be different in phantoms with higher F contents shown in table 2. Figure 3 illustrates the F calibration line.

The MDL was found to be 0.54 g F. To convert it to the MDL in the unit of concentration, the mass of the sample needs to be considered. The mass of cortical bone of a reference man is found to be 54 g (ICRP 1975). So the MDL in terms of concentration is calculated to be 10 mg F g^{-1} bone. Using a conversion factor of 3.68 g bone g^{-1} Ca (Woodard 1964), the MDL would be 36.8 mg F g^{-1} Ca.

The levels of F in human bone were found to be between 1.1–11.6 mg F g^{-1} Ca (Mostafaei *et al* 2015b), which is lower than the MDL calculated from this study. However, the DD neutron generator with higher flux is available which can lower the detection limit down to the normal range of F in human bones.

Dose calculation

The dose received by the patient is a main limiting factor for the *in vivo* measurements. One goal of this study was to obtain highest sensitivity for bone F measurement with the lowest dose possible. The Monte Carlo simulation (MCNPX) was used to determine the hand and whole body dose. The equivalent dose to the hand during the 20 s irradiation time with 7×10^8 n s^{-1} neutron flux was found to be 0.9 mSv. The effective dose outside the cavity was calculated to be 38.8 μSv h^{-1}, and 0.22 μSv for 20 s of irradiation. The effective dose contributed by the hand was calculated using the Monte Carlo simulation results, while taking the hand weighting factor (0.01) and weight of the hand to the whole body (0.0125) into account. The effective dose contributed by the hand was found to be 0.11 μSv. By adding the dose outside the shielding assembly with the hand effective dose, the whole body effective dose was calculated to be 0.33 μSv. This is lower in comparison to standard routine medical imaging procedures (e.g. a chest x-ray whole body dose is 100 μSv). Also, the annual natural background radiation exposure level in North America is approximately 3000 μSv (ICRP 1991).

Adding a multiplier and moderator to the system

In order to improve the MDL and detect the lowest F level in people, some further optimization was investigated. The system optimization using MCNP simulation by adding different beryllium (Be) and polyethylene thicknesses (0–6 cm) as a multiplier and moderator before the existing 5 cm polyethylene moderator inside the irradiation box was investigated. The 500 ppm F phantom was simulated and the number of counts and doses for each Be and polyethylene thicknesses were investigated separately.

The neutron beam is pre-moderated and multiplied by beryllium filters via the $^{9}Be(n,2n)^{8}Be$ reaction in order to have a lower energy source for *in vivo* measurements. This leads to better thermalization of the neutron beam and a lower dose per unit activation to the person being measured. Adding Be thicknesses as a multiplier has shown to increase the activation in comparison to polyethylene.

Figure 4(a) shows the different activations with various Be and polyethylene thicknesses. Also, the ratio of F counts over dose with various thicknesses of Be and polyethylene is shown in figure 4(b). Although the number of F counts were increased by approximately 14.4% when the Be thickness was used instead of polyethylene, the irradiation dose to the subject increases by 37%. This is not considered an advantage. However, further simulations

are being performed to optimize the combination of various Be and polyethylene thicknesses, which could increase the number of counts with a minimal increase of dose.

Discussion

In previous studies, the NAA technique using the Tandem accelerator at McMaster University shows that a reasonably low detection limit, 0.17 mg F g^{-1} Ca, could be achieved for an equivalent dose to the irradiated hand of 30 mSv. This is a comparable dose to that received by patients during clinical examinations (Mostafaei *et al* 2013b). F levels in hand bone for a group of healthy volunteers measured by that system was found to be 1.1–11.6 mg F g^{-1} Ca (Chamberlain *et al* 2012a, 2012b, Mostafaei *et al* 2013b, 2015b). The McMaster Tandem accelerator has shown to be well thermalized, and the thermal neutron flux was found to be 9×10^8 n cm^{-2} s^{-1} in the center of the irradiation cavity (Mostafaei *et al* 2015a). The thermal neutron flux was found to be much lower with the DD generator used in this study in comparison with the Tandem accelerator.

To obtain a sufficiently high flux of thermal neutrons in the irradiation cavity, a DD generator with a higher flux would be preferred. Using an advanced DD generator with higher neutron flux up to 2×10^{10} n s^{-1}, which is a factor of 30 higher than the current study, the MDL would decrease by a factor of √30 (from 36.8 mg F g^{-1} Ca to 6.7 mg F g^{-1} Ca) assuming that the background under the F gamma ray peak increase linearly with the neutron flux. In our measurements, the increase of the background is much lower than the increase of the flux, so the factor would be between √30 and 30. Based on Fordyce study in 2011 F concentration in bone divides into three phases; normal (0.5–1 mg F g^{-1} bone ash), preclinical (3.5–5.5 mg F g^{-1} bone ash) and clinical phase I (6–7 mg F g^{-1} bone ash) (Fordyce *et al* 2011). Using the conversion factor of 2.5 g bone ash g^{-1} Ca (ICRP 1975), the MDL extrapolated from the worst-case scenario can be converted to 2.7 mg F g^{-1} bone ash (i.e. the MDL would be lower than this value given the extrapolation factor of greater than √30). The bone F in subjects at the categories of ‘preclinical phase’ and ‘clinical phase I’ will be observed. The F in the subjects at ‘normal phase’ might also be observed.

The numbers of counts obtained experimentally from the F phantoms were found to be different from the simulations in higher concentrations. This might be due to the time uncertainty of transferring the F phantoms from irradiation system to detection system. The short half-life of F makes each second of transferring time critical. Also, a higher neutron flux was observed with the DD generator during the F phantom measurements with higher concentrations. The neutron flux was calculated to be 7×10^8 n s^{-1} in previous study (Liu *et al* 2014). But the generator was manufactured with the neutron flux as up to 3×10^9 n s^{-1}. The neutron flux can be adjusted by changing the acceleration voltage and ion current. For F phantom measurements acceleration voltage and ion current were set at 120 KV and 16 mA. Further investigation with high concentration of F phantom and the fluctuation in neutron flux is needed.

Further improvements can be made by: i) an addition of high efficiency HPGe detector to reduce the MDL by detecting more γ-rays, ii) using a DD system with higher neutron flux,

iii) an optimized moderator, reflector, multiplier and shielding assembly to generate more thermal neutrons but stay within the acceptable dose range.

Easy transfer and minimal space needed are considered the main advantages of the compact DD neutron generator in comparison to McMaster's accelerator. This advantage will warrant the future goal of developing the IVNAA technology for measuring patients with a DD neutron generator.

Conclusion

A feasibility study using Monte Carlo simulation and experiments has been performed on the potential use of a compact DD neutron generator system for the determination of bone F concentration. It is predicted that using an advanced high flux DD generator with optimized moderator, multiplier and reflector, the system could detect the levels of bone F with an acceptable radiation dose in a population in the 'preclinical phase' and 'clinical phase I'. Future studies include development of such a system for bone F measurement using a high flux DD generator and application of the technology in human studies on health effect of F exposure.

Acknowledgment

This work was supported by the National Institute for Occupational Safety and Health (NIOSH) R21 grants 1R21OH010044 and 1R21OH010700, the Purdue University Nuclear Regulatory Commission (NRC) Faculty Development Grant NRC-HQ-11-G-38-0006, and Purdue Bilsland Fellowship.

References

ATSDR 2003 Toxicological profile for fluorides, hydrogen fluoride, and fluorine Agency for Toxic Substances and Disease Registry, Public Health Service (Atlanta, GA: US Department of Health and Human Services) (www.atsdr.cdc.gov/toxprofiles/tp11.html)

Augenstein WL, Spoerke DG, Kulig KW, Hall AH, Hall PK, Riggs BS, Saadi ME and Rumack BH 1991 Fluoride ingestion in children: a review of 87 cases Pediatrics 88 907–12 [PubMed: 1945630]

Bevington PR 2003 Data Reduction and Error Analysis for Physical Sciences 3rd edn (New York: McGraw-Hill)

Boivin G, Chavassieux P, Chapuy MC, Baud CA and Meunier PJ 1989 Skeletal fluorosis: histomorphometric analysis of bone changes and bone fluoride content in 29 patients Bone 10 89–99 [PubMed: 2765315]

Burt BA 1992The changing patterns of systemic fluoride intake J. Dent. Res 71 1228–37 [PubMed: 1607439]

Chamberlain M et al. 2012a The feasibility of *in vivo* quantification of bone-fluorine in humans by delayed neutron activation analysis: a pilot study Physiol. Meas 33 243–57 [PubMed: 22273740]

Chamberlain M et al. 2012b *In vivo* quantification of bone-fluorine by delayed neutron activation analysis: a pilot study of hand-bone-fluorine levels in a Canadian population Physiol. Meas 33 375–84 [PubMed: 22369953]

Chettle DR 2006 Occupational nuclear medicine: trace element analysis of living human subjects J. Radioanal. Nucl. Chem 268 653–61

Chettle DR and Fremlin JH 1984 Techniques of *in vivo* neutron activation analysis Phys. Med. Biol 29 1011–43 [PubMed: 6385030]

Fordyce FM and Nriagu JO 2011 Fluorine: Human Health Risks Encyclopedia of Environmental Health vol 2 (Burlington: Elsevier) pp 776–85

Hibbert DB and Gooding JJ 2006 Data Analysis for Chemistry (New York: Oxford University Press)

ICRP 1975 Report of the Task Group on Reference Man (Publication No.23) (New York: International Commission on Radiological Protection)

ICRP 1991 Recommendations of the international commission on radiological protection Ann. ICRP 21 1–201

ICRP 2002 Basic anatomical and physiological data for use in radiological protection: reference values. A report of age- and gender-related differences in the anatomical and physiological characteristics of reference individuals Ann. ICRP 32 5–265 [PubMed: 14506981]

Johnson HJE, Kearns AE, Doran PM, Khoo T and Wermers RA 2007 Fluoride-related bone disease associated with habitual tea consumption Mayo Clin. Proc. Mayo Clin 82 719–24 [PubMed: 17550752]

Kaminsky LS, Mahoney MC, Leach J, Melius J and Miller MJ 1990 Fluoride: benefits and risk of exposure Oral Biol. Med 1 261–81

Khandare AL, Harikumar R and Sivakumar B 2005 Severe bone deformities in young children from vitamin D deficiency and fluorosis in Bihar-India Calcif. Tissue Int 76 412–8 [PubMed: 15895280]

Krishnan SS, Mernagh JR, Hitchman AJW, McNeill KG and Harrison JE 1985 Measurements of fluoride in bone biopsies by neutron activation analysis for the clinical study of osteoporosis Nucl. Chem 95 119–25

Kurland ES, Schulman RC, Zerwekh JE, Reinus WR, Dempster DW and Whyte MP 2007 Case Report J. Bone Miner. Res 22 163–70 [PubMed: 17014382]

Limeback H 1999 A re-examination of the pre-eruptive and post-eruptive mechanism of the anti-caries effects of fluoride: is there any anti-caries benefit from swallowing fluoride? Community Dent. Oral Epidemiol 27 62–71 [PubMed: 10086928]

Liu Y, Byrne P, Wang H, Koltick D, Zheng W and Nie LH 2014 A compact DD neutron generator-based NAA system to quantify manganese (Mn) in bone *in vivo* Physiol. Meas 35 1899–911 [PubMed: 25154883]

Liu Y, Koltick D, Byrne P, Wang H, Zheng W and Nie LH 2013 Development of a transportable neutron activation analysis system to quantify manganese in bone *in vivo*: feasibility and methodology Physiol. Meas 34 1593–609 [PubMed: 24165395]

Ludlow M, Luxton G and Mathew T 2007 Effects of fluoridation of community water supplies for people with chronic kidney disease Nephrol. Dialysis Transplantation 22 2763–7

Mostafaei F, McNeill FE, Chettle DR, Prestwich WV and Inskip M 2013a Design of a phantom equivalent to measure bone-fluorine in a human's hand via delayed neutron activation analysis Physiol. Meas 34 503–12 [PubMed: 23587669]

Mostafaei F, McNeill FE, Chettle DR and Prestwich WV 2013b Improvements in an *in vivo* neutron activation analysis (NAA) method for the measurement of fluorine in human bone Physiol. Meas 34 1329 [PubMed: 24045335]

Mostafaei F, McNeill FE, Chettle DR, Matysiak W, Bhatia C and Prestwich WV 2015a An investigation of the neutron flux in bone-fluorine phantoms comparing accelerator based *in vivo* neutron activation analysis and FLUKA simulation data Nucl. Instrum. Methods Phys. Res. B 342 249–57

Mostafaei F, McNeill FE, Chettle DR, Wainman BC, Pidruczny AE and Prestwich WV 2015b Measurements of fluorine in contemporary urban Canadians: a comparison of the levels found in human bone using *in vivo* and *ex vivo* neutron activation analysis Physiol. Meas 36 465–87 [PubMed: 25669130]

Nie LH, Sanchez S, Grodzins L, Cleveland R and Weisskopf MG 2011 *In vivo* quantification of lead in bone with a portable XRF system—methodology and feasibility Phys. Med. Biol 56 N39–51 [PubMed: 21242629]

Phipps KR 1996 Fluoride Present Knowledge in Nutrition 7th edn ed Ziegler EE and Filer LJ Jr (Washington, DC: ILSI Press) pp 329–33

Shashi A, Kumar M and Bhardwaj M 2008 Incidence of skeletal deformities in endemic fluorosis Tropical doctor 38 231–3 [PubMed: 18820194]

Sowers D, Liu Y, Mostafaei F, Blake S and Nie LH 2015 A dosimetry study of deuterium-deuterium neutron generator-based *in vivo* neutron activation analysis Health Phys. J (at press)

Susheela AK, Bhatnagar M and Vig K 2005 Excess fluoride ingestion and thyroid hormone derangement in children living in Delhi, India Fluoride 38 98–108

Tamer MN, Kale Köroğlu B, Arslan C, Akdoğan M, Köroğlu M, Cam H and Yildiz M 2007 Osteosclerosis due to endemic fluorosis Sci. Total Environ 373 43–8 [PubMed: 17182085]

Tilley DR, Cheves CM, Kelley JH, Raman S and Weller HR 1998 Energy levels of light nuclei Nucleonics 636 249–364

Turner CH, Hasegawa K, Zhang W, Wilson M, Li Y and Dunipace AJ 1995 Fluoride reduces bone strength in older rats J. Dent. Res 74 1475–81 [PubMed: 7560402]

Wang W et al. 2007 Thoracic ossification of ligamentum flavum caused by skeletal fluorosis Eur. Spine J 16 1119–28 [PubMed: 17075705]

Wilson J 1993 Endemic skeleton: patients fluorosis radiographic of the features Am. Roentgen Ray Soc 94–98

Whitford GM 1989 The Metabolism and Toxicity of Fluoride (Basel, Switzerland: Karger)

Whitford GM 1990 The physiological and toxicological characteristics of fluoride J. Dent. Res 69 539–49 [PubMed: 2179312]

Whitford GM 1994 Intake and metabolism of fluoride Adv. Dent. Res 8 5–14 [PubMed: 7993560]

Woodard HQ 1964 The composition of human cortical bone Clin. Orthop. Relat. Res 37 187–93 [PubMed: 5889132]

Yadav AK, Kaushik CP, Haritash AK, Singh B, Raghuvanshi SP and Kansal A 2007 Determination of exposure and probable ingestion of fluoride through tea, toothpaste, tobacco and pan masala J. Hazardous Mater 142 77–80

Zipkin I, McCcaps FJ and Lee WA 1960 Relation of the fluoride content of human bone to its chemical composition Arch. Oral Biol 2 190–5 [PubMed: 13788623]

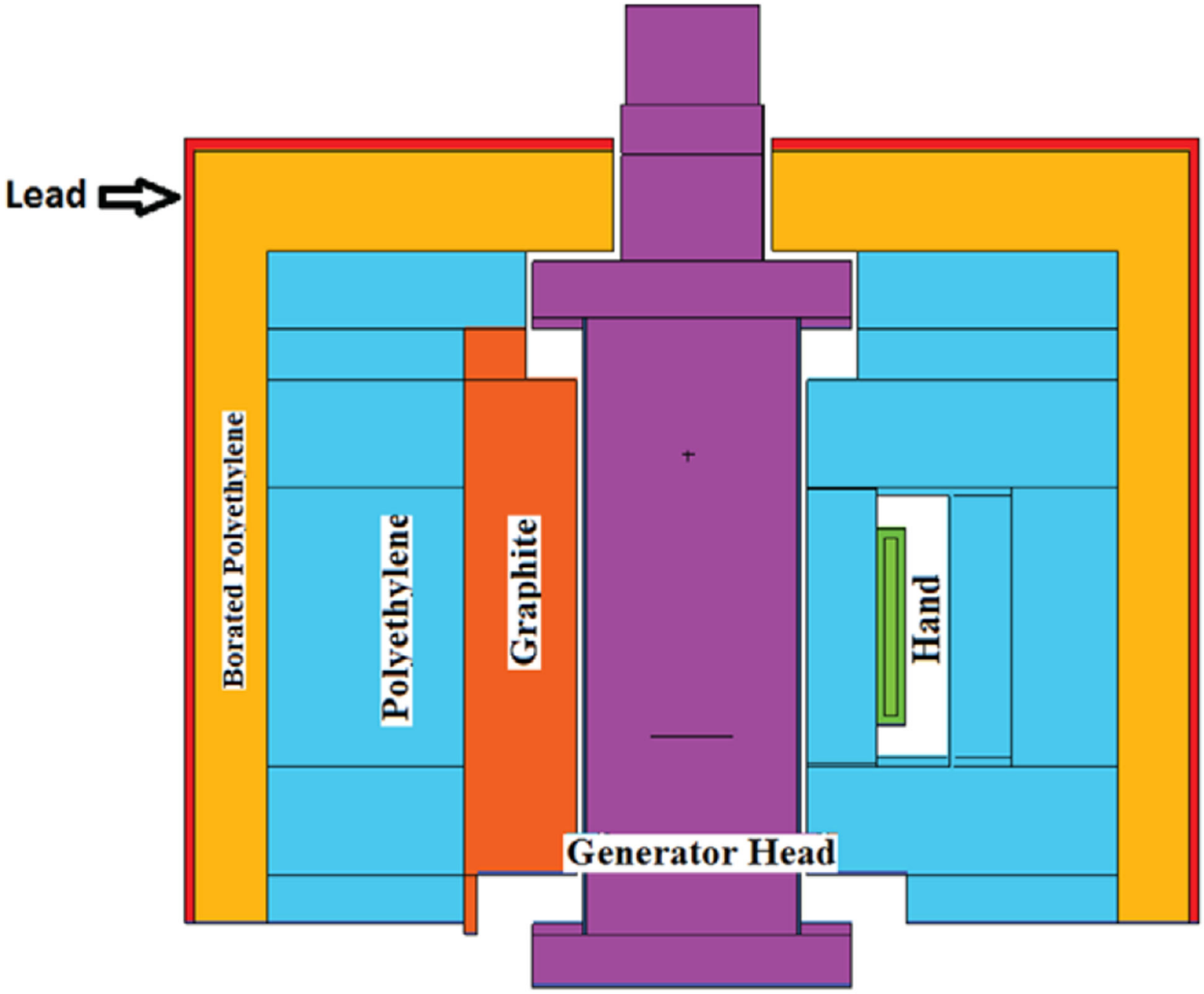

Figure 1.
A cross-section of the generator head, moderator, reflector, shielding, and irradiation zone.

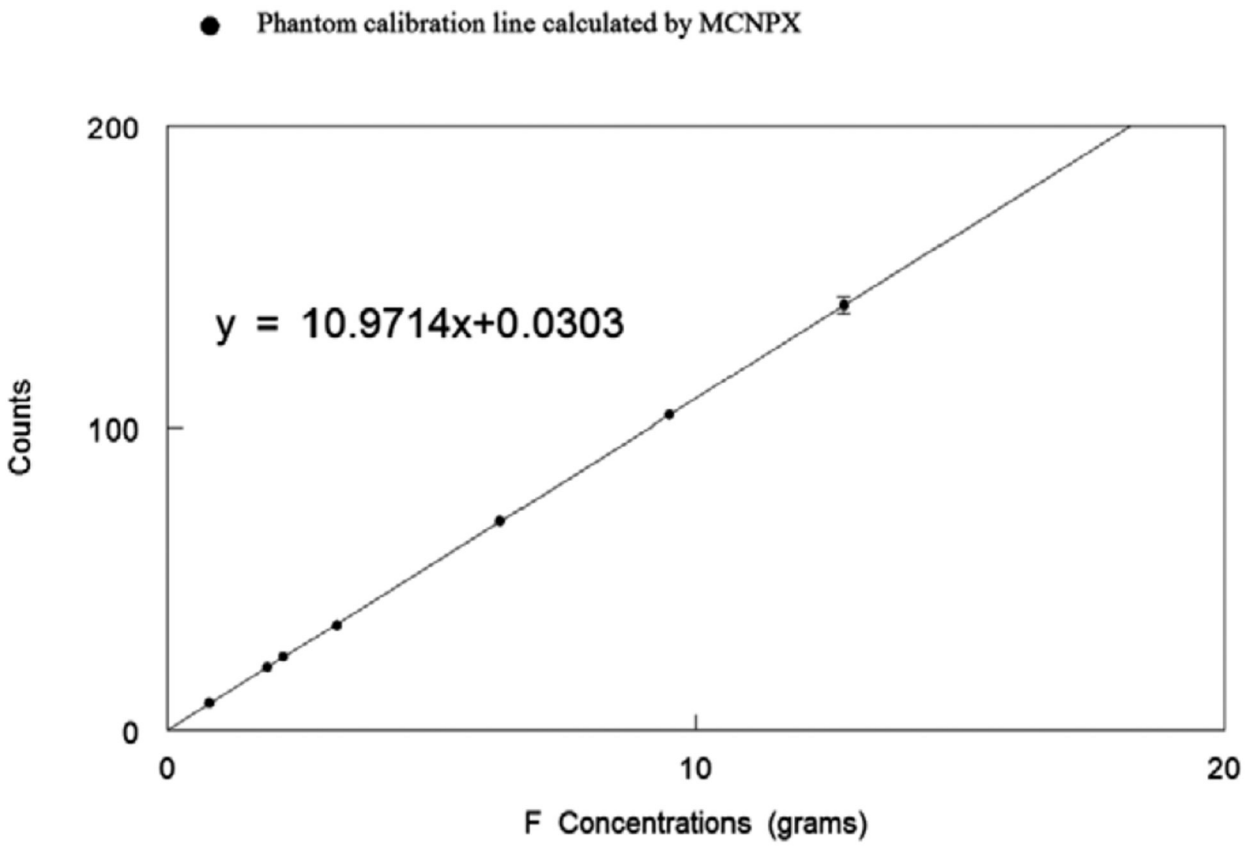

Figure 2.
Phantom calibration line calculated by MCNPX.

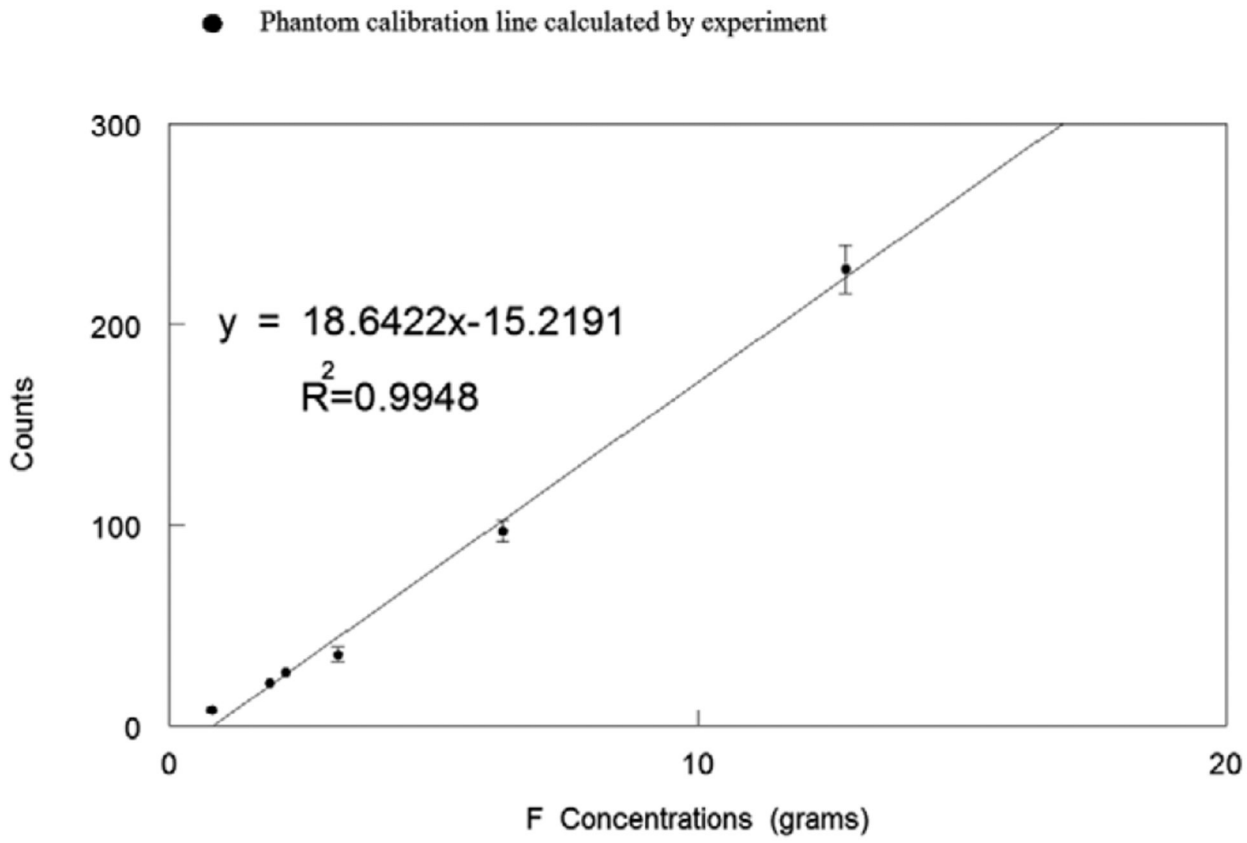

Figure 3.
The F phantom calibration line with the experiment.

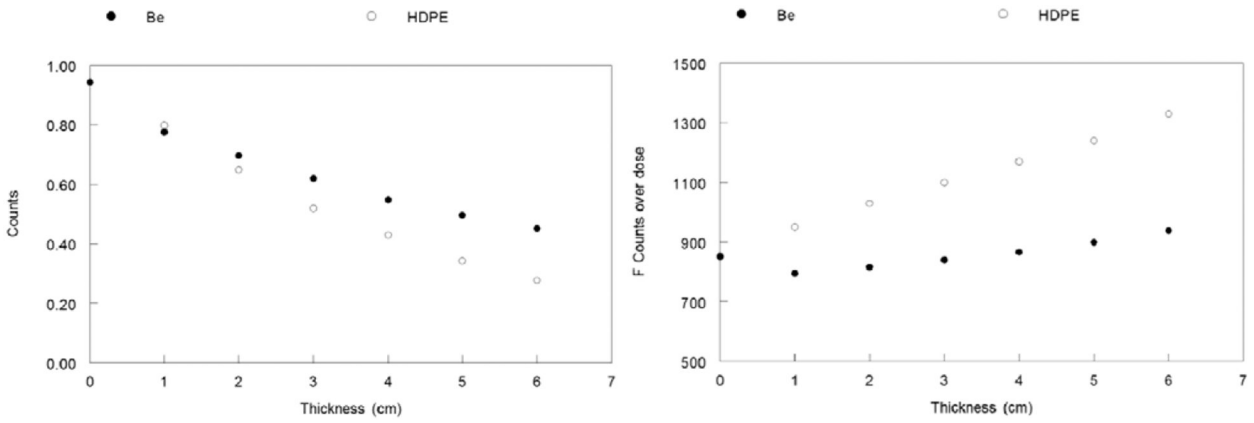

Figure 4.

(a) Number of F counts with different Be and HDPE thicknesses, (b) The ratio of F counts over dose.

Table 1.

Number of counts calculated by MCNPX.

***F* (grams)**	**0.82**	**1.9**	**2.2**	**3.2**	**6.3**	**9.5**	**12.8**
Counts	9.0 ± 0.2	20.8 ± 0.4	24.3 ± 0.5	34.7 ± 0.7	69.3 ± 1.4	104.2 ± 2.1	140.5 ± 2.8

Table 2.

Number of counts calculated by experiments.

***F* (grams)**	**0.82**	**1.9**	**2.2**	**3.2**	**6.3**	**12.8**
Counts	7.8 ± 2.8	21.5 ± 2.6	26.7 ± 2.6	35.4 ± 3.8	96.9 ± 5.5	227.4 ± 11.9